



# A Comprehensive Prognostic and Immunological Analysis of a Six-Gene Signature Associated With Glycolysis and Immune Response in Uveal Melanoma

Jun Liu<sup>1,2†</sup>, Jianjun Lu<sup>3,4†</sup> and Wenli Li<sup>1\*</sup>

<sup>1</sup> Reproductive Medicine Center, Yue Bei People's Hospital, Shantou University Medical College, Shaoguan, China, <sup>2</sup> Medical Research Center, Yue Bei People's Hospital, Shantou University Medical College, Shaoguan, China, <sup>3</sup> Department of Medical Affairs, First Affiliated Hospital of Sun Yat-sen University, Guangzhou, China, <sup>4</sup> The Second School of Clinical Medicine, Southern Medical University, Guangzhou, China

## OPEN ACCESS

### Edited by:

Niels Schaft,  
University Hospital Erlangen, Germany

### Reviewed by:

Suman Mitra,  
UMR1277 Hétérogénéité, Plasticité et  
Résistance aux Thérapies  
Anticancéreuses (CANTHER)  
(INSERM), France  
Amitabha Chaudhuri,  
MedGenome Inc., United States

### \*Correspondence:

Wenli Li  
wangyiliwenli@163.com

<sup>†</sup>These authors share first authorship

### Specialty section:

This article was submitted to  
Cancer Immunity  
and Immunotherapy,  
a section of the journal  
Frontiers in Immunology

**Received:** 08 July 2021

**Accepted:** 02 September 2021

**Published:** 22 September 2021

### Citation:

Liu J, Lu J and Li W (2021) A  
Comprehensive Prognostic and  
Immunological Analysis of a Six-Gene  
Signature Associated With Glycolysis  
and Immune Response  
in Uveal Melanoma.  
*Front. Immunol.* 12:738068.  
doi: 10.3389/fimmu.2021.738068

Uveal melanoma (UM) is a subtype of melanoma with poor prognosis. This study aimed to construct a new prognostic gene signature that can be used for survival prediction and risk stratification of UM patients. In this work, transcriptome data from the Molecular Signatures Database were used to identify the cancer hallmarks most relevant to the prognosis of UM patients. Weighted gene co-expression network, univariate least absolute contraction and selection operator (LASSO), and multivariate Cox regression analyses were used to construct the prognostic gene characteristics. Kaplan–Meier and receiver operating characteristic (ROC) curves were used to evaluate the survival predictive ability of the gene signature. The results showed that glycolysis and immune response were the main risk factors for overall survival (OS) in UM patients. Using univariate Cox regression analysis, 238 candidates related to the prognosis of UM patients were identified ( $p < 0.05$ ). Using LASSO and multivariate Cox regression analyses, a six-gene signature including *ARPC1B*, *BTBD6*, *GUSB*, *KRTCAP2*, *RHBDD3*, and *SLC39A4* was constructed. Kaplan–Meier analysis of the UM cohort in the training set showed that patients with higher risk scores had worse OS (HR = 2.61,  $p < 0.001$ ). The time-dependent ROC (t-ROC) curve showed that the risk score had good predictive efficiency for UM patients in the training set (AUC > 0.9). Besides, t-ROC analysis showed that the predictive ability of risk scores was significantly higher than that of other clinicopathological characteristics. Univariate and multivariate Cox regression analyses showed that risk score was an independent risk factor for OS in UM patients. The prognostic value of risk scores was further verified in two external UM cohorts (GSE22138 and GSE84976). Two-factor survival analysis showed that UM patients with high hypoxia or immune response scores and high risk scores had the worst prognosis. Moreover, a nomogram based on the six-gene signature was established for clinical practice. In addition, risk scores were related to the immune infiltration profiles. Taken together, this study identified a new prognostic six-gene signature related to glycolysis and immune

response. This six-gene signature can not only be used for survival prediction and risk stratification but also may be a potential therapeutic target for UM patients.

**Keywords:** uveal melanoma, overall survival, glycolysis, immune response, gene signature

## INTRODUCTION

Uveal melanoma (UM) is a rare and aggressive intraocular malignant tumor, and about 50% of patients are prone to liver metastases. The prognosis of metastatic UM is poor, and there is a lack of effective treatments. The average incidence per year is 5.1 per million people, which ranks first among intraocular tumors (1). About 90% of UMs are located in the choroid. Increased ocular melanocytes, choroidal nevi, and *BRCA1*-associated protein 1 mutations are considered to be risk factors for the occurrence of UM (2). The clinicopathological characteristics (such as the diameter of the basal tumor, ciliary body involvement, and scleral expansion), non-random chromosomal aberrations, gene mutations (such as *BAP1* and *SF3B1* mutations) are considered to be related to the prognosis of patients with UM (3–5). Recent studies have shown that percutaneous hepatic perfusion can control the progression of UM metastatic intrahepatic lesions (6). Meanwhile, early surgical treatment of UM liver metastases may help improve the progression-free survival (PFS) and overall survival (OS) in UM patients with liver metastases (7–11). Therefore, early diagnosis and surgical treatment are essential to improve the prognosis of patients with UM (12, 13).

Therefore, screening new survival predictors is of great significance for guiding the diagnosis and treatments of UM. However, on the one hand, the predictive ability of traditional clinicopathological features such as pathological staging has been shown to be insufficient. On the other hand, previous studies have used global gene expression data to build signatures that are likely to bring gene sets from different biological processes, masking the key biological features driving prognosis. Therefore, our approach was to start with the biological processes relevant in UM and construct signatures around the same to create a gene signature with fewer genes than those constructed in earlier studies.

Previous studies have shown that cancer hallmarks, such as glycolysis and immune response, are associated with the prognosis of UM patients (14, 15). As is known, immunotherapy can induce an immune response in certain cancers to help control cancer progression. However, due to reasons such as the lack of *BRAF* mutations and loss of *BAP1* expression, the response rate of UM to immune checkpoint blockade is very low (16). Studies have shown that the high density of tumor-associated macrophages and infiltrating T lymphocytes in UM is related to the poor prognosis of UM patients (17). Therefore, although the mutation burden of UM is low, it does have immunogenicity. This is of great significance to the development of immunotherapy (18). Therefore, the prognostic gene signature constructed using the gene sets of immune response may be more related to the immune cell infiltration status and help discover potential targets for immunotherapy in UM.

In this study, we extracted an UM cohort from The Cancer Genome Atlas (TCGA), screened out the most important prognostic genes related to the two cancer hallmarks, glycolysis and immune response, and established a UM survival prediction gene signature. Subsequently, the prognostic value of the risk model based on the gene signature was verified in two independent UM validation sets from the Gene Expression Omnibus (GEO) database. Next, the prognostic values of the risk models and cancer markers (such as glycolysis and immune response) were further analyzed. A time-dependent receiver operating characteristic (t-ROC) curve was used to verify the predictive accuracy of the gene signature. In addition, the correlation between the risk model and the tumor immune microenvironment (TIME) was explored. In conclusion, this study constructed a new prognostic gene signature related to cancer hallmarks, including glycolysis and immune response, for patients with UM. This gene signature could help develop individualized treatment plans for patients with UM and may be expected to serve as a potential prognostic biomarker for UM.

## MATERIAL AND METHODS

### Dataset Preparation and Data Processing

The UM dataset containing the messenger RNA (mRNA) expression profiles and clinical information of 80 UM patients obtained from TCGA database (<http://cancergenome.nih.gov/>) was used as the training dataset for establishing the prognostic model. The validation datasets GSE22138 and GSE84976, with the UM-mRNA expression profiles and clinical information downloaded from the GEO (<http://www.ncbi.nlm.nih.gov/geo/>) database, included 63 and 28 UM patients, respectively. The two above-mentioned databases are publicly available. Therefore, this study did not require the approval of the local ethics committee.

### Candidate Selection and Gene Signature Establishment

Using the transcriptome profiling data and hallmark gene sets from the Molecular Signatures Database (MSigDB) and the single-sample gene set enrichment analysis (ssGSEA) (R package “gsva”), the performance of the cancer hallmarks in the training set was quantified for univariate Cox proportional hazards (Cox-PH) regression analysis to evaluate the significance of various cancer hallmarks in UM (R package “survival”) (19, 20). Weighted gene co-expression network analysis (WGCNA) was used to construct a scale-free co-expression network (R package “wgcna”) to identify the gene module most relevant to glycolysis and immune response based on data from the transcriptome analysis and the ssGSEA scores (21). Meanwhile,

the correlations between individual genes and the ssGSEA scores of the cancer hallmarks were quantified by gene significance (GS); the correlations between module characteristic genes and the gene expression profiles were represented by module members (MM). Using the *p*-value threshold of GS <0.0001 and the significance threshold of univariate Cox regression with *p* < 0.01, 238 genes extracted from the module as most related to glycolysis and immune response were screened as candidates. Next, the least absolute shrinkage and selection operator (LASSO) Cox regression model was used to further screen the most reliable prognostic biomarkers (22). Specifically, univariate Cox regression analysis was conducted to identify genes related to OS, and then LASSO Cox regression was applied to further narrow the scope of the UM marker genes. In terms of the calculation principle, LASSO regression can not only solve the overfitting problem but also extract useful features by directly reducing some repeated unnecessary parameters to zero in the parameter reduction process. Subsequently, multiple Cox regression analysis was performed to evaluate whether marker genes can be used as independent prognostic factors for patient survival. Next, WGCNA was used to construct a gene co-expression network. The risk model related to glycolysis and immune response was established by including standardized gene expression values weighted by its LASSO Cox coefficient. The formula is as follows:

$$\text{Risk score} = \sum_i \text{Coefficient (mRNA}_i\text{)} * \text{Expression (mRNA}_i\text{)}$$

### Survival Analysis Based on the Risk Model

Taking the median risk score as the cutoff value, we divided the UM patients into a high-risk and a low-risk group. Subsequently, the prognosis of the two groups was compared. The ROC curve was used to evaluate the prediction accuracy of the risk model. Moreover, a two-factor survival analysis combining the risk scores and cancer hallmarks (such as glycolysis and immune response) was conducted in the training set and the validation set GSE22138 to comprehensively evaluate the impact of risk scores and cancer hallmarks on the prognosis of UM patients.

### Robustness of the Six-Gene Signature in UM

To confirm the prognostic values of the genes from another perspective, six genes were randomly selected from the UM transcriptome data for evaluation of their prognostic performance. This process was repeated 1,000 times to increase statistical power. In addition, previous studies have constructed some gene signatures that can be used to predict the survival of UM patients. For example, a 10-gene signature constructed to predict the survival of UM patients showed good survival predictive ability (23). Therefore, in order to further explore the prognostic significance of the gene signature constructed in this study, we compared the predictive power of five gene signatures for UM patients.

### Prognostic Value of the Gene Signature in Other Tumors

In order to fully understand the prognostic value of our gene signature in tumors, we evaluated its ability to predict survival in other tumors. As is known, skin melanoma (SM) is another subtype of melanoma and hepatocellular carcinoma (HCC) is a visceral tumor. Therefore, SM and HCC were used as the cancer

types to evaluate the survival predictive ability of our gene signature in tumors other than UM.

### Establishment and Evaluation of Survival Prediction Nomogram for UM Patients

Nomogram is an effective method for predicting the prognosis of cancer patients by simplifying complex statistical prediction models into contour maps that assess the probability of OS of individual patients (24). In this study, we constructed a nomogram based on the six-gene signature to evaluate the probability of OS in UM patients at 1, 3, and 5 years. Meanwhile, the predicted probability of the nomogram is compared with the observed actual probability through a calibration curve in order to verify the accuracy of the nomogram. An overlap with the reference line indicates that the model is accurate.

### Correlation Analysis Between Risk Scores and TIME

The immune-related complex environment for the survival and development of tumor cells is described as the tumor microenvironment. In this study, four analysis methods, namely, TIMER, CIBERSORT, quanTIseq, and xCELL, were applied to analyze the correlations between the risk scores and immune cell infiltration status. Heat maps and bar graphs were drawn to compare the immune infiltration levels of the various immune cells in the high- and low-risk groups. Furthermore, we performed a two-factor survival analysis combining the immune cell infiltration levels and the risk scores. In addition, this study explored the correlation between the risk scores and some immune checkpoint molecules.

### Bioinformatics and Statistical Analysis

GSEA using the glycolysis and immune response genome from MSigDB was performed to verify the glycolysis and immune response status of the high-risk group (25). IBM SPSS Statistics 20 (IBM Corp., Armonk, NY, USA) and R software (version 3.5.2; <http://www.r-project.org>) were used to analyze the data and draw charts. The *Z*-score method was utilized to normalize the ssGSEA scores and the risk scores based on the gene signature. The Kaplan–Meier method was employed to draw the survival curve and the log-rank test used to assess differences between groups. The Cox-PH regression model was used to evaluate the importance of each parameter to OS. The t-ROC analysis was performed to measure the predictive power of the risk model (R package “survival-ROC”) (26). The areas under the ROC curve of the various variables at different time points (AUC-t) were compared. The “wilcox.test” function was applied to compare the risk scores of the two groups; the “kruskal.test” function was used to compare the risk scores of the different pathological stages.

## RESULTS

### Schematic Diagram of the Study Design

**Figure 1** displays the flowchart of the entire work. The figure shows the detailed construction process of the prediction model

in predicting the OS of patients with UM. At the start, glycolysis and immune response are identified as the primary cancer hallmarks for survival in UM. Next, WGCNA, univariate and multivariate Cox regression analyses, and the LASSO algorithm were employed to identify the hub genes related to glycolysis and immune response. Furthermore, the identified hub genes were used to establish the risk model predicting the OS of UM patients. Subsequently, the prognostic value of the risk model was evaluated in the training set and in two independent validation sets. Information of the patients in TCGA and the GEO cohorts is shown in **Table 1**.

## Glycolysis and Immune Response Were Identified as the Primary Risk Factors for OS of UM Patients

According to the ssGSEA scores and survival information of the cancer hallmarks in the training set, the Cox coefficient of each cancer hallmark was calculated and sorted. Univariate analysis suggested that, compared with the other cancer hallmarks such as PI3K/AKT/mTOR signaling, apoptosis, EMT, G2M checkpoint, TGF-beta signaling, angiogenesis, and hypoxia, glycolysis and immune response were the most significant risk factors affecting the survival of UM patients (**Figure 2A**). Multivariate analysis suggested that glycolysis and immune response were independent prognostic factors for OS of UM patients (**Figure 2B**). As shown in **Figure 2C**, the glycolysis and immune response Z-scores of UM patients who died during follow-up were significantly higher than those of patients who are still alive. Subsequently, taking the median of the risk score as the cutoff value, we divided the 80 UM patients in the training set into a high-risk group and a low-risk group. Survival analysis suggested that the OS rate of the group with high glycolysis Z-scores was lower than that of the group with low glycolysis Z-

scores [hazard ratio (HR) = 7.46,  $p < 0.001$ ] (**Figure 2D**). Meanwhile, the OS rate of the group with high immune response Z-scores was lower than that of the group with low immune response Z-scores (HR = 6.83,  $p < 0.001$ ) (**Figure 2E**).

## Establishment of Prognostic Gene Signature Related to Glycolysis and Immune Response

WGCNA was performed using the whole-transcriptome analysis data and the ssGSEA Z-scores of glycolysis and immune response in the training set. A total of seven non-gray modules were generated (**Figure 3A**). Among these modules, the green module had the highest correlation with glycolysis and immune response ( $r > 0.5$ ,  $p < 0.0001$ ) (**Figure 3B**). With a  $p$ -value threshold for GS of  $< 0.0001$ , the hub genes extracted from the green module were used for univariate Cox regression analysis. With a  $p$ -value threshold for univariate Cox regression of  $< 0.01$ , 238 candidates with prognostic values were screened out (**Figure 3C**). Subsequently, LASSO Cox regression was performed to determine the most robust prognostic biomarkers. By applying a 10-fold cross-validation to overcome overfitting, nine variables were identified (**Figures 3D, E**). With multivariate Cox stepwise regression analysis, six hub genes were identified for constructing a prognostic risk model for UM patients: risk score =  $3.80 * ARPC1B + 4.02 * BTBD6 + 1.02 * GUSB + 2.10 * KRTCAP2 - 6.65 * RHBDD3 + 2.25 * SLC39A4$ .

## Risk Score Is an Independent Risk Factor for OS of Patients with UM in the Training Set

As shown in **Figure 4A**, the proportion of patients who died during follow-up in the high-risk group was higher than that in the low-risk group in the training set. **Figure 4B** shows that the risk scores of patients who died during follow-up were

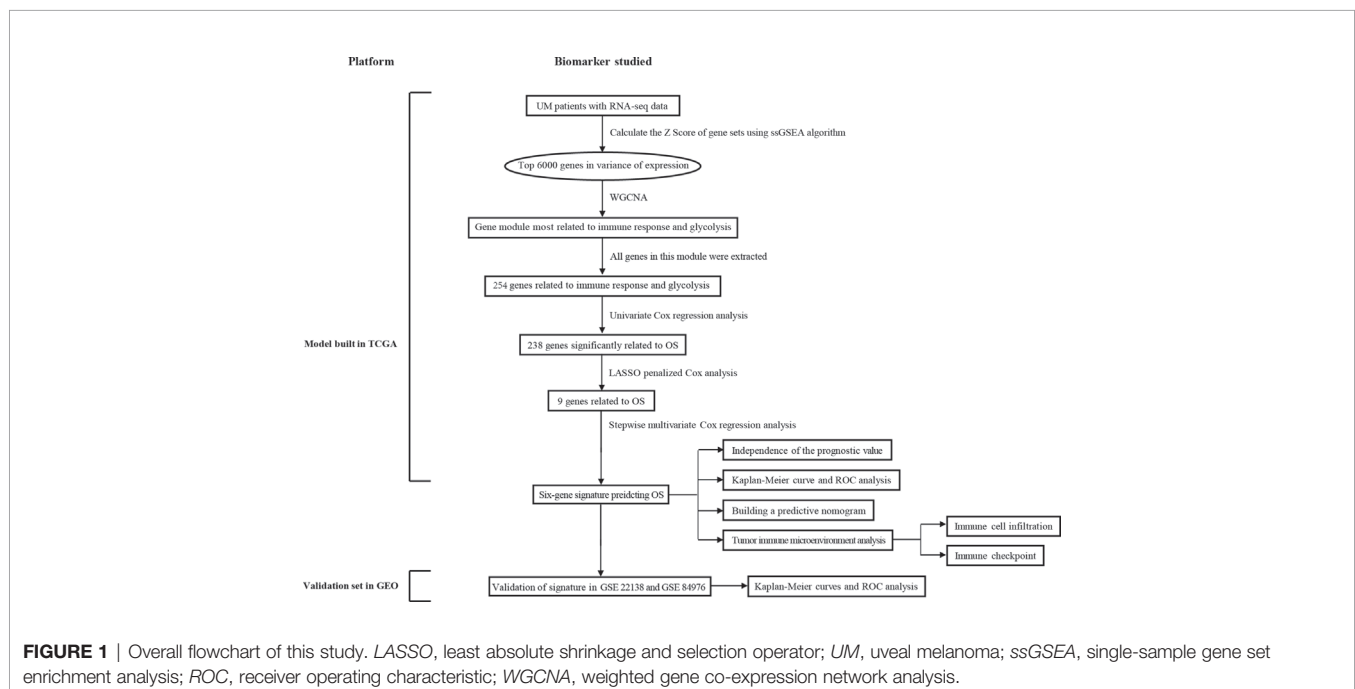


**FIGURE 1** | Overall flowchart of this study. LASSO, least absolute shrinkage and selection operator; UM, uveal melanoma; ssGSEA, single-sample gene set enrichment analysis; ROC, receiver operating characteristic; WGCNA, weighted gene co-expression network analysis.

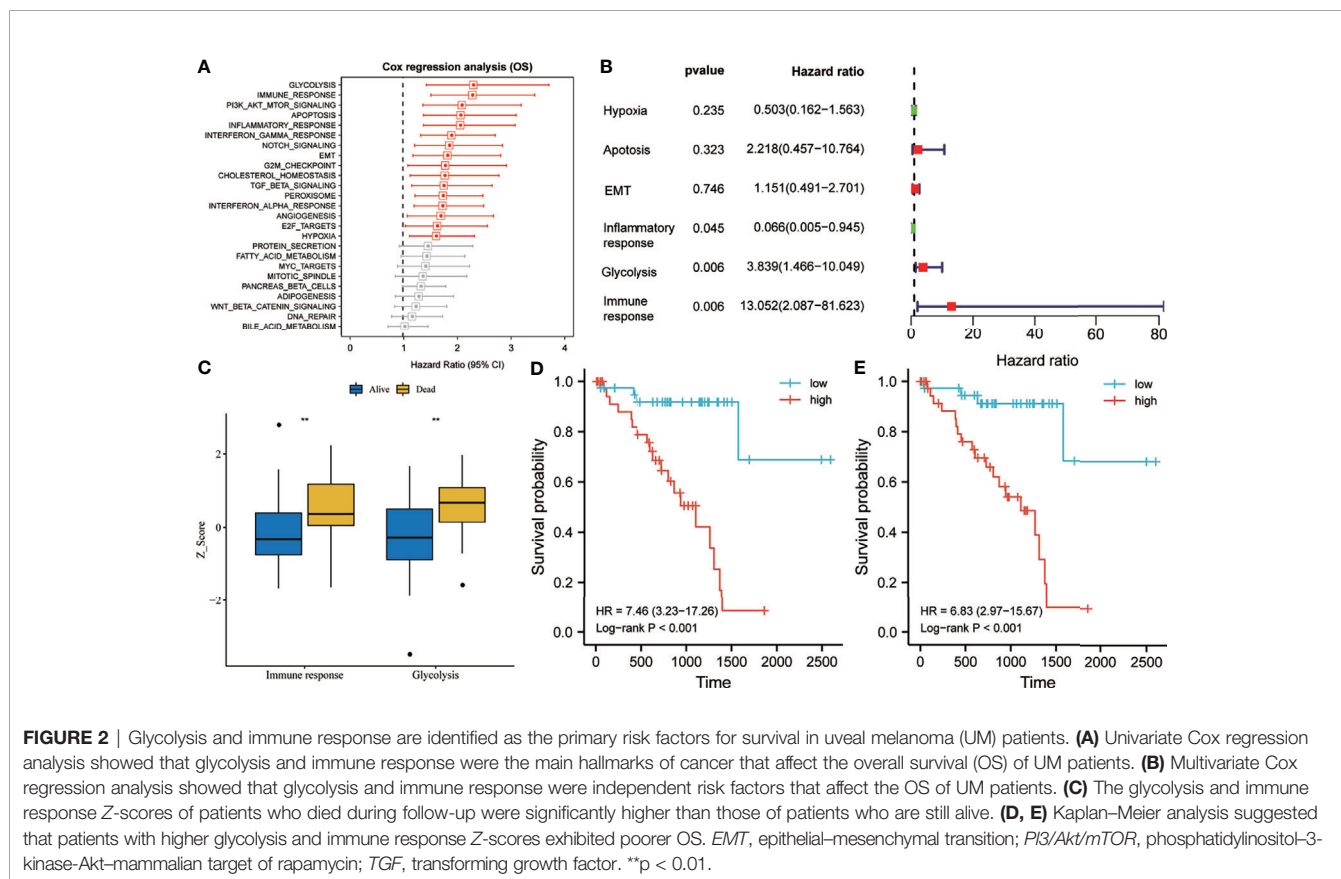
**TABLE 1** | Baseline demographic and clinical information in The Cancer Genome Atlas (TCGA) and the Gene Expression Omnibus (GEO) cohorts.

Clinical characteristics		Total	%
TCGA			
Status	Alive	57	71.25
	Dead	23	28.75
Age (years)	<60	36	45
	≥60	44	55
Sex	Female	35	43.75
	Male	45	56.25
T	T2	14	17.5
	T3	32	40
	T4	34	42.5
Stage	Stage II	36	45
	Stage III	40	50
	Stage IV	4	5
GSE22138			
Status	Alive	28	44.44
	Dead	35	55.56
Age (years)	<60	28	44.44
	≥60	35	55.56
Sex	Female	24	38.1
	Male	39	61.9
GSE84976			
Status	Alive	12	42.86
	Dead	16	57.14
Age (years)	<60	12	42.86
	≥60	16	57.14

significantly higher than those of patients who are still alive. In addition, patients with more advanced pathological stages had higher risk scores (**Figure 4C**). Kaplan–Meier analysis showed that patients with higher risk scores had a worse prognosis than did patients with lower risk scores (HR = 23.85,  $p < 0.001$ ) (**Figure 4D**). The ROC curve showed that the AUCs of risk scores predicting the 1-, 2-, 3-, 4-, and 5-year survival rates were above 0.9, suggesting that risk score was a good model for predicting the survival of UM patients (**Figure 4E**). At the same time, multivariate Cox regression analysis suggested that, among the various clinicopathological variables in the training set, risk score was an independent risk factor for OS (HR = 2.61,  $p < 0.001$ ) (**Figure 4F**).

### Risk Score Is a Risk Factor for Disease Progression in the Training Set

As shown in **Figure 5A**, the proportion of patients with disease progression in the high-risk group was higher than that in the low-risk group in the training set. **Figure 5B** shows that the risk scores of patients with disease progression during follow-up were significantly higher than those of disease-free patients. Kaplan–Meier analysis showed that the PFS of the high-risk group was worse than that of the low-risk group (HR = 7.21,  $p < 0.001$ ) (**Figure 5C**). The ROC curve showed that the AUCs of risk scores



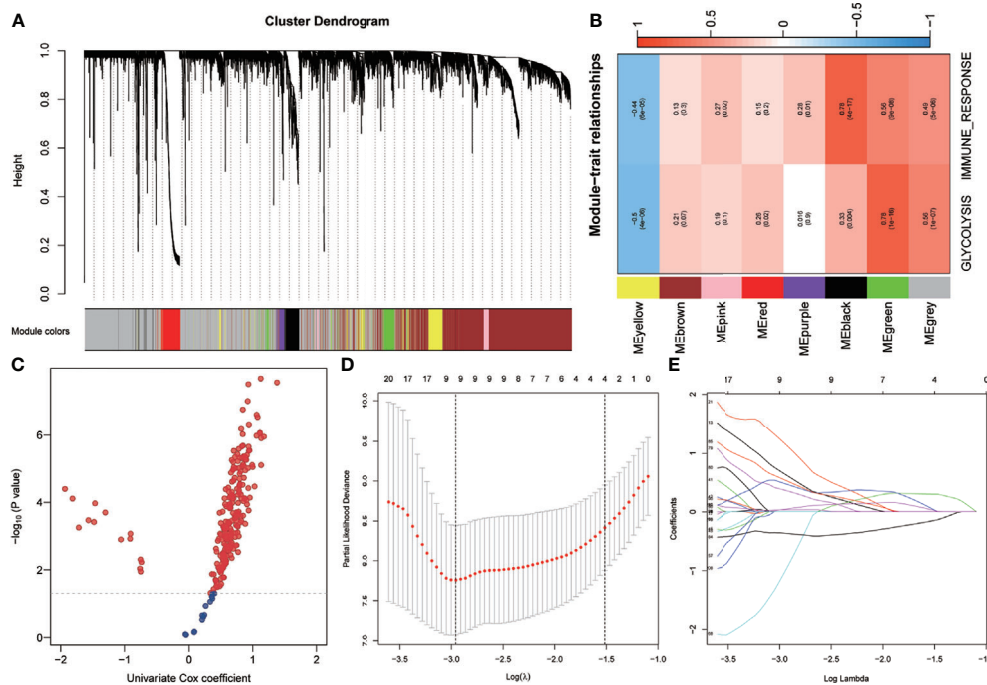


**FIGURE 3** | Establishment of genetic signatures related to glycolysis and immune response. **(A)** The variance of the expression value of each gene in the training set was calculated, and then the top 6,000 genes in the variance ranking were used to construct the WGCNA network. Seven non-gray modules were identified. **(B)** The green module depicting the highest correlation ( $r > 0.5$ ,  $p < 0.0001$ ) was considered the most correlated with glycolysis and immune response. **(C)** Using univariate Cox regression analysis, 238 prognostic-related candidate genes were extracted from the key genes from the green module. **(D, E)** The LASSO Cox regression model was used to identify the most robust biomarkers, and multivariate Cox stepwise regression was applied to construct a prognostic model. LASSO, minimum absolute shrinkage and selection operator; WGCNA, weighted gene co-expression network analysis.

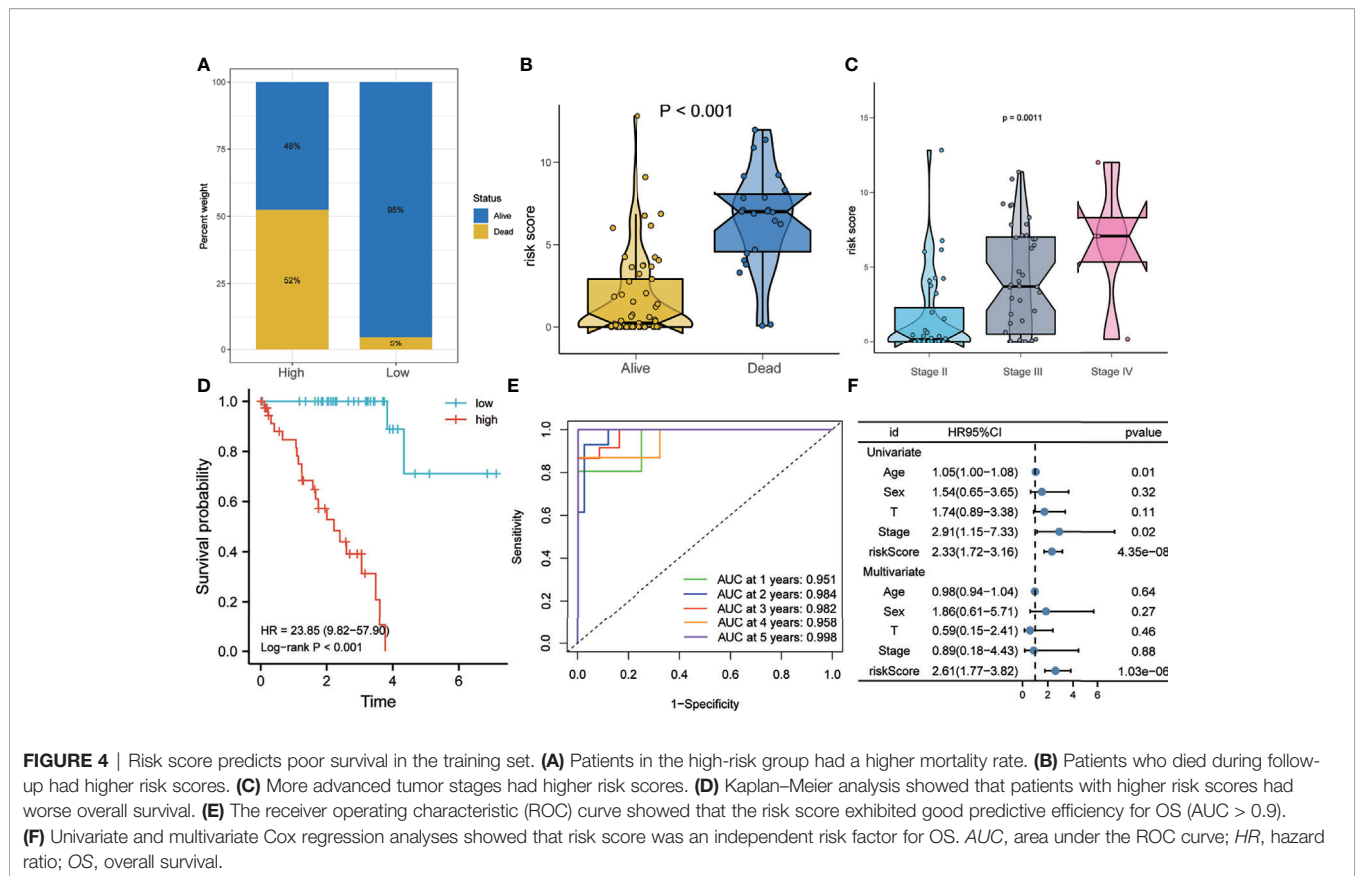
predicting the 1-, 2-, 3-, 4-, and 5-year survival rates were above 0.8, suggesting that risk score was a good model for predicting PFS in UM patients (**Figure 5D**). Meanwhile, multivariate Cox regression analysis suggested that, among the various clinicopathological variables in the training cohort, risk score was an independent risk factor for PFS (HR = 1.47,  $p < 0.001$ ) (**Figure 5E**). In addition, the t-ROC analysis suggested that risk score was an accurate indicator for predicting PFS (**Figure 5F**).

In order to further verify the robustness of the risk model in predicting the survival of UM patients, it was validated in independent external UM cohorts. As shown in **Figure 6A**, the proportion of patients who died in the high-risk group was higher than that in the low-risk group. **Figure 6B** shows that the risk scores of patients who died were significantly higher than those of patients who are still alive ( $p < 0.0001$ ). Kaplan–Meier analysis suggested that the OS of the high-risk group was worse than that of the low-risk group (HR = 3.87,  $p < 0.001$ ) (**Figure 6C**). The ROC curve showed that the AUCs of risk scores predicting the 1-, 2-, 3-, 4-, and 5-year survival rates were above 0.7, suggesting that risk score was a good model for predicting the OS of UM patients (**Figure 6D**). Multivariate Cox regression analysis suggested that, among the various clinicopathological variables, risk score was an independent risk factor for OS (HR = 1.41,  $p < 0.001$ ) (**Figure 6E**). In addition, t-ROC analysis suggested that risk score was an accurate indicator for predicting the OS of UM patients (**Figure 6F**).

Similarly, as shown in **Figure 7A**, the proportion of patients who died in the high-risk group was higher than that in the low-risk group. **Figure 7B** shows that the risk score of patients who died during follow-up was significantly higher than that of patients who are still alive ( $p < 0.0001$ ). Kaplan–Meier analysis showed that the OS of the high-risk group was worse than that of the low-risk group (HR = 17.01,  $p < 0.001$ ) (**Figure 7C**). In addition, the ROC curve showed that the AUCs of risk scores for predicting the 1-, 2-, 3-, 4-, and 5-year survival rates were all above 0.8, suggesting that risk score was a good model for predicting the OS of UM patients (**Figure 7D**).

### Correlation of Risk Scores With Cancer Hallmarks, Including Glycolysis and Immune Response, and Corresponding Two-Factor Survival Analysis

The results of the two-factor survival analysis combining the risk scores and cancer hallmarks in the training set are shown in **Figure 8**. The high-risk group had higher glycolytic and immune response Z-scores (**Figure 8A**). UM patients with low risk scores and low glycolytic or immune response Z-scores showed the best OS, while those with high risk scores and high glycolytic or immune response Z-scores showed a worse prognosis (**Figures 8B, C**). Using differentially expressed gene (DEG) analysis, a total of 814 DEGs, including 259



downregulated and 555 upregulated genes, were identified [with  $|\log_2FC| > 1$ , false discovery rate (FDR)  $< 0.05$  as the cutoff value] (**Figure 8D**). In addition, the Kyoto Encyclopedia of Genes and Genomes (KEGG) analysis showed that the main enrichment pathways of these DEGs included phagosome, Epstein–Barr virus infection, cell adhesion molecules, human T-cell leukemia virus 1 infection, human cytomegalovirus infection, cytokine–cytokine receptor interaction, tuberculosis, *Staphylococcus aureus* infection, antigen processing and presentation, and Th1 and Th2 cell differentiation (**Figure 8E**). Meanwhile, the results of the two-factor survival analysis combining the risk scores and cancer hallmarks in the validation set (GSE22138) are shown in **Figure S1**. The high-risk group had higher immune response and glycolytic Z-scores (**Figure S1A**). UM patients with low risk scores and low immune response or glycolytic Z-scores showed the best OS, while those with high risk scores and high immune response or glycolytic Z-scores showed a worse prognosis (**Figures S1B, C**).

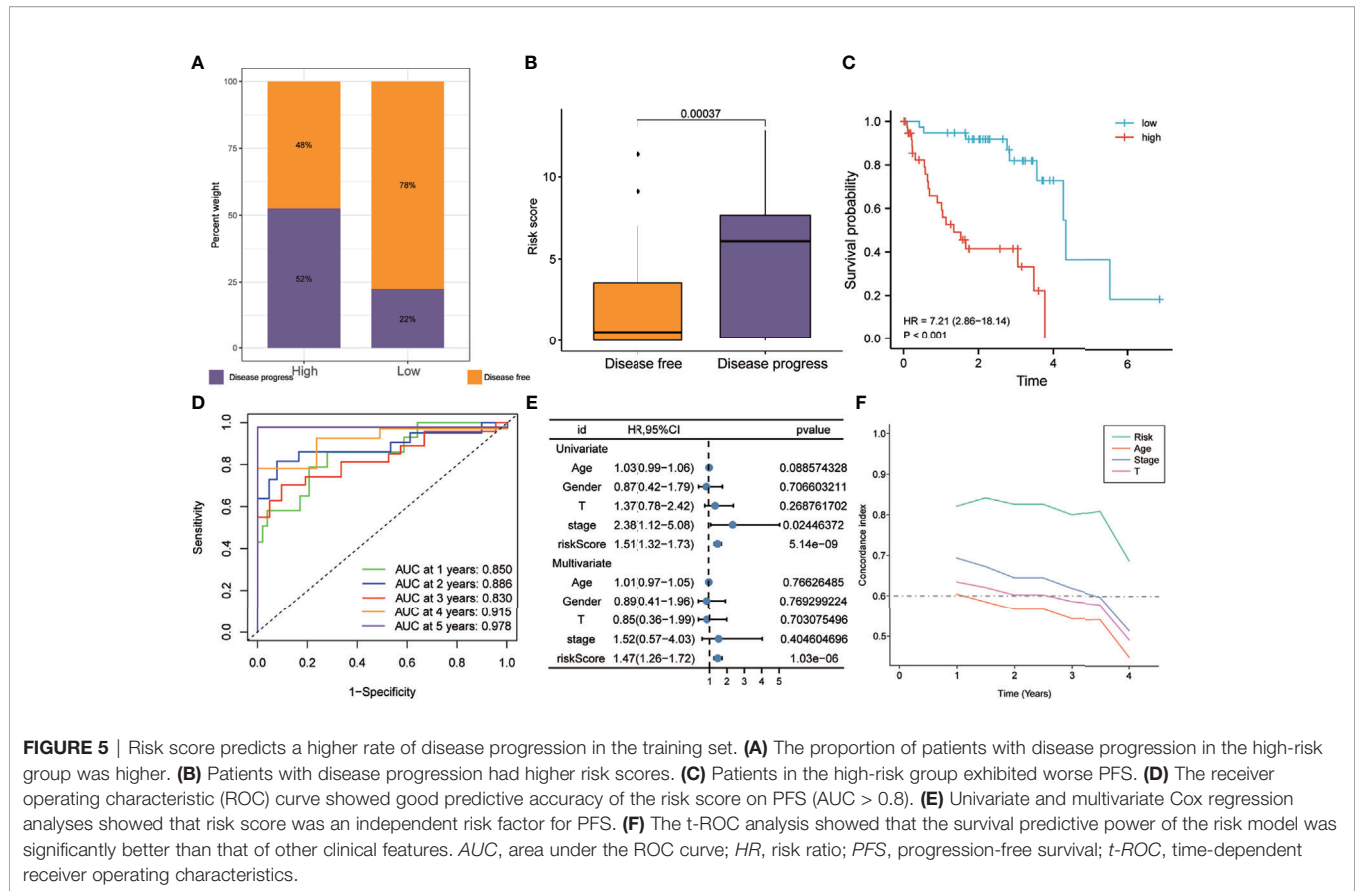
## The Six-Gene Signature Is a Good Predictive Model With Fewer Genes

In order to confirm the predictive ability of the six-gene signature constructed in this study from another perspective, six genes were randomly selected from the UM transcriptome data for evaluation of the prognostic performance. As shown in **Table S1**, 1,000 randomly selected six-gene combinations failed to predict the survival of UM patients. These results further confirmed the predictive ability of the six-gene signature. In addition, we

considered that a comparison of the predictive abilities of various gene signatures for UM patients could help to further explore the prognostic values of these gene signatures. Therefore, the predictive abilities of five gene signatures were compared. The five included signatures are defined as follows: 1) the six-gene signature constructed in this study; 2) the 10-gene signature (*SIRT3*, *HMCES*, *SLC44A3*, *TCTN1*, *STPG1*, *POMGNT2*, *RNF208*, *ANXA2P2*, *ULBP1*, and *CA12*) constructed by Luo et al. (23); 3) the 16-gene signature constructed by combining the six-gene and 10-gene signatures; 4) the five-gene signature (*ANXA2P2*, *CA12*, *HMCES*, *SIRT3*, and *SLC44A3*) constructed by performing stepwise multifactor Cox regression analysis on the 10-gene signature; and 5) the random six-gene signature constructed by randomly selecting six genes from the UM transcriptome data. As shown in **Figures S2A, B**, the t-ROC analysis and the concordance index (C-index) analysis showed that the 6-gene, 10-gene, 16-gene, and 5-gene signatures had good survival predictive capabilities (AUC > 0.85). The prediction results of these four gene signatures were well consistent with the survival results actually observed in UM. In addition, the random six-gene signature failed to predict survival in UM (AUC < 0.57).

## The Survival Prediction Ability of the Six-Gene Signature in UM Was Much Better Than That in SM and HCC

In order to further explore the prognostic value of the six-gene signature in tumors, we evaluated its predictive ability for OS in



SM and HCC. Kaplan–Meier analysis showed that SM patients with higher risk scores had a worse prognosis than those with lower risk scores (HR = 1.56,  $p = 0.001$ ) (Figure S2C). However, the ROC curves showed that the predictive ability of the six-gene signature in SM was low (AUC < 0.63) (Figure S2D). Similarly, HCC patients with higher risk scores had a worse prognosis than those with lower risk scores (HR = 1.74,  $p = 0.002$ ) (Figure S2E). Also, the predictive ability of the six-gene signature in HCC was low (AUC < 0.66) (Figure S2F). These results indicate that the survival predictive ability of the six-gene signature in UM was much better than that in SM and HCC.

## Building a Nomogram to Predict OS in UM Patients

We constructed a nomogram for clinical practice based on the six-gene signature (Figure S3A). Then, a calibration curve was created to verify the predictive ability of the nomogram (Figure S3B). The calibration chart showed that the predicted 1-, 3-, and 5-year survival probabilities were in good agreement with the actual observations.

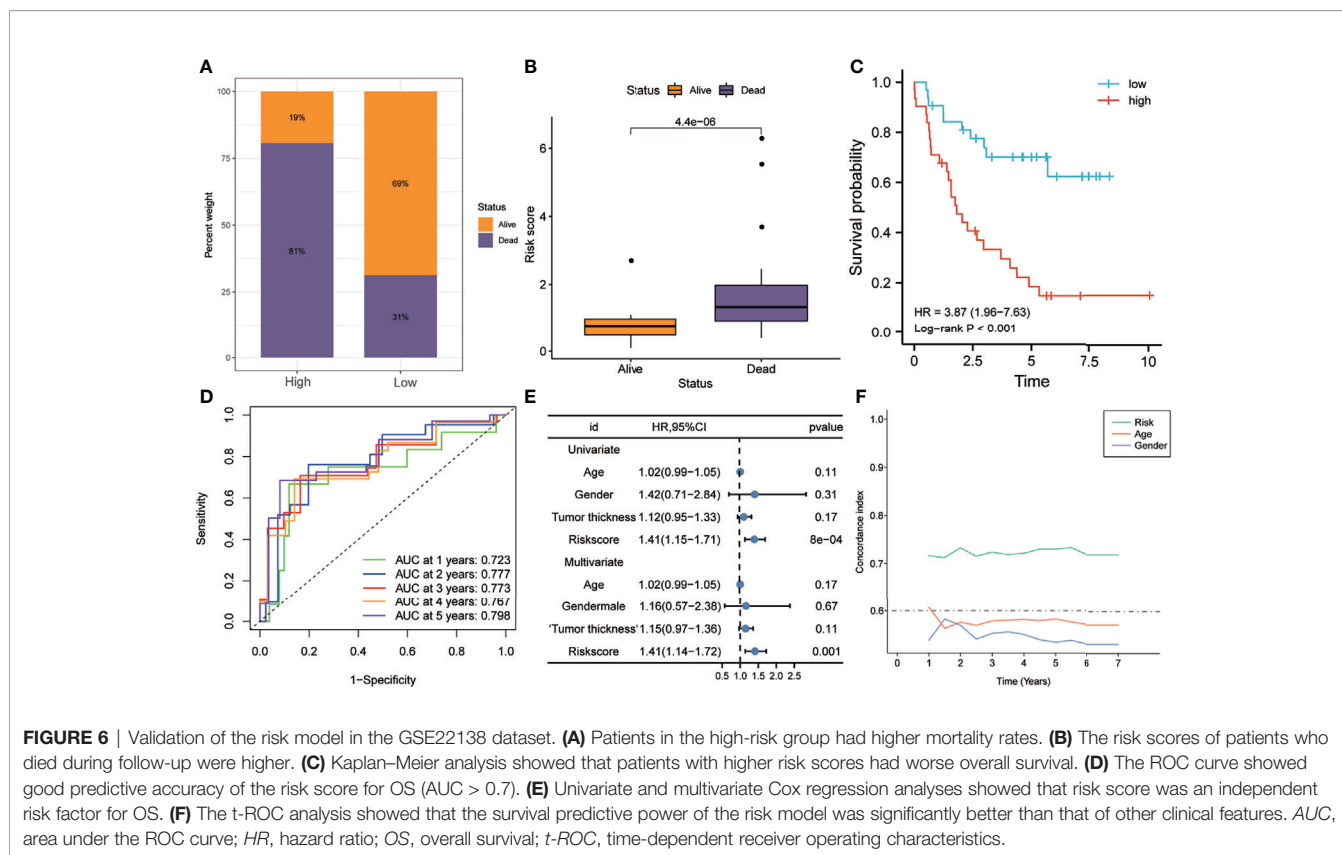
## Correlation Analysis Between Risk Score and the Immune Cell Infiltration Profiles

A heat map was drawn to detect the correlations between the risk scores and the levels of immune cell infiltration. Four methods were applied in this study: TIMER, CIBERSORT, quanTIseq, and

xCELL. As shown in Figure 9A, the results of TIMER suggest that the infiltration levels of B cells and CD4<sup>+</sup> T cells were higher in the low-risk group. The results from CIBERSORT showed that the infiltration levels of B cells, CD4<sup>+</sup> T cells, and monocytes were higher in the low-risk group. Meanwhile, the results from quanTIseq showed that the immune infiltration levels of M2 macrophages were higher in the high-risk group. The results of xCELL suggested that the immune infiltration levels of myeloid dendritic cells were higher in the high-risk group. Moreover, immune checkpoints are sensitive molecules expressed by immune cells that can regulate immune activation. Therefore, we explored the correlations between the risk scores and the expression levels of various immune checkpoint molecules. The results suggested that the expression levels of immune checkpoint molecules such as *CD27*, *CD48*, *CD86*, *HAVCR2*, *ICOS*, and indoleamine 2,3-dioxygenase 1 (*IDO1*) were significantly correlated (Figure 9B).

## UM Patients With High Risk Scores and Low Immune Cell Scores Showed Poor OS

Immune cell infiltration in the tumor microenvironment affects the prognosis of tumor patients. Therefore, this study explored the correlations between the risk scores and the infiltration status of various immune cells. The results from TIMER suggested that the risk score was significantly related to the infiltration level of immune cells such as B cells, CD8 T cells, and myeloid dendritic



cells (**Figure S4A**). The results from CIBERSORT suggested that the risk score was significantly correlated with the infiltration level of immune cells such as CD8 T cells, monocytes, and activated mast cells (**Figure S4B**). The results of quantIseq suggested that the risk score was significantly related to the infiltration levels of immune cells such as M2 macrophages, natural killer (NK) cells, regulatory T cells, CD4 T cells, CD8 T cells, and myeloid dendritic cells (**Figure S4C**). The results of xCELL suggested that the risk score was significantly related to the infiltration levels of immune cells such as central memory CD8<sup>+</sup> T cells, common myeloid progenitors, macrophages, M2 macrophages, NK cells, and Th2 CD4 T cells (**Figure S4D**). The two-factor survival analysis combining the immune cell scores and risk scores showed that UM patients with low risk scores and high immune cell scores showed better OS, while those with high risk scores and low immune cell scores showed poor OS (**Figures S4E–H**).

## DISCUSSION

UM is a malignant tumor with poor prognosis. Early diagnosis and treatment are of great significance for improving the survival of patients with UM. However, there is currently a lack of accurate prognostic biomarkers for UM. Previous studies have shown that cancer hallmarks such as glycolysis and immune response are related to the prognosis of UM patients (14, 15).

Therefore, this study focused on constructing a gene signature with prognostic values related to glycolysis and immune response. Firstly, using ssGSEA and Cox-PH regression models, glycolysis and immune response were identified as the cancer hallmarks most relevant to the OS of UM patients. Then, using WGCNA, the gene module most related to glycolysis and immune response was identified. Next, using univariate, LASSO, and multivariate regression analyses, hub genes (including *ARPC1B*, *BTBD6*, *GUSB*, *KRTCAP2*, *RHBDD3*, and *SLC39A4*) with prognostic values from the gene module were identified. Finally, the survival analysis results in the training and validation sets confirmed that this six-gene signature is an independent prognostic predictor of OS for patients with UM. Furthermore, we established a nomogram based on the six-gene signature that can be used in clinical practice.

As is known, the occurrence and progression of many human cancers are related to cancer hallmarks such as immune response, and immunotherapy has curative effects on certain cancers (27–29). It has been reported that immune cells such as CD8<sup>+</sup> T cells, monocytes, memory CD4<sup>+</sup> T cells, and mast cells are significantly related to the OS of UM patients (30). Moreover, some immune-related gene signatures related to the survival of UM patients have been identified (15). Immune checkpoints such as TIGIT and IDO are considered as potential therapeutic targets for UM patients (31). However, the low immunogenicity of UM greatly limits the application of immunotherapy on UM (32–34). It is worth mentioning that recent studies have suggested that adoptively

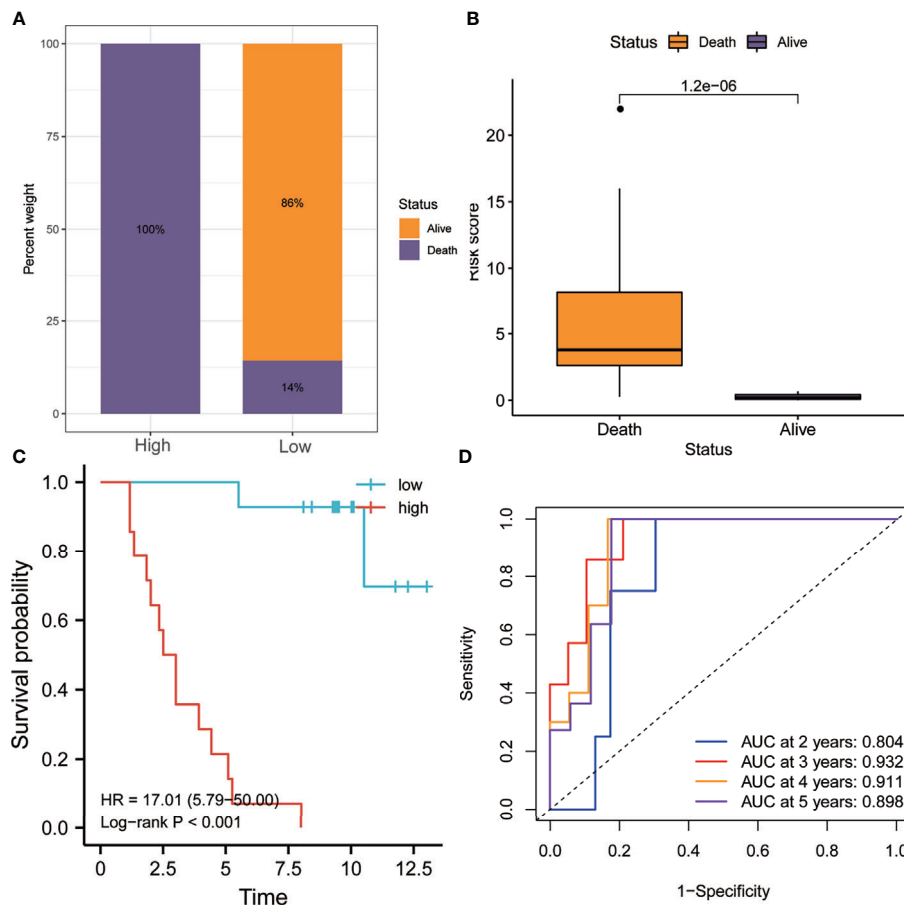
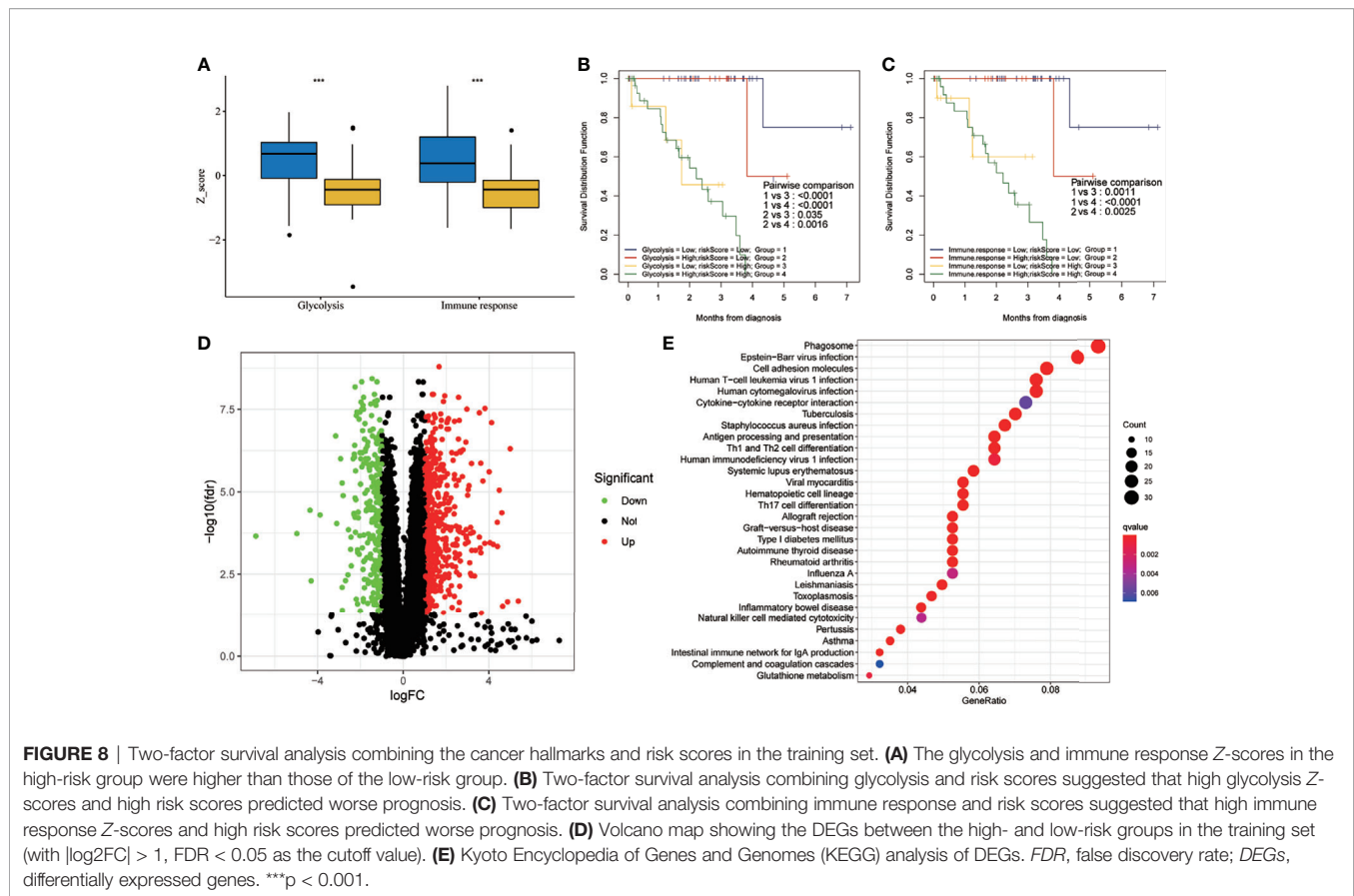


**FIGURE 7** | Validation of the risk model in the GSE84976 dataset. **(A)** Patients in the high-risk group had higher mortality rates. **(B)** The risk scores of patients who died during follow-up were higher. **(C)** Kaplan-Meier analysis showed that patients with higher risk scores had worse overall survival. **(D)** The receiver operating characteristic (ROC) curve showed good predictive accuracy of the risk score for OS (AUC > 0.8). AUC, area under the ROC curve; HR, hazard ratio; OS, overall survival.

transferred tumor-infiltrating lymphocytes have shown curative effects on metastatic UM (27). In addition, PD-L1 is expressed in 10% of UM, and anti-PD-1-based treatment may bring clinical benefits to patients with metastatic UM (35, 36). Blood biomarkers such as lactate dehydrogenase (LDH), C-reactive protein (CRP), and relative eosinophil count (REC) can be used to predict the survival prognosis of patients treated with immune checkpoint blockade (37). Therefore, this study explored the correlation between this prognostic six-gene signature and immune cell infiltration. The results showed that the infiltration levels of B cells, CD4<sup>+</sup> T cells, and monocytes in the low-risk group were higher. At the same time, the infiltration levels of M2 macrophages and myeloid dendritic cells in the high-risk group were higher. Two-factor survival analysis combining the immune cell scores and risk scores showed that UM patients with low risk scores and high immune cell scores showed better OS, while patients with high risk scores and low immune cell scores showed worse OS. Therefore, this six-gene signature may provide potential targets for immunotherapy of UM.

One of the important clinical characteristics of UM is the possibility of metastasis in the early stages of tumor development. However, the current traditional clinicopathological staging has limited predictive power for the prognosis of UM (38). Therefore, new therapeutic targets and immunomodulatory methods are urgently needed to improve the therapeutic effect and prognosis of patients with UM (39). Some studies have shown that microRNAs (miRNAs) such as miR-195, miR-224, miR-365a, miR-365b, miR-452, miR-4709, miR-7702, miR-513c, miR-873, miR-506-514 cluster, miR-592, and miR-199a are related to the OS of UM patients (40, 41). Meanwhile, some changes in the miRNA expression may be used to identify metastatic UM. Some changes in the miRNA expression in metastatic UM may be potential therapeutic targets (42). In addition, m6A RNA methylation regulators could also be used to assess the prognosis of patients with UM (43). As an effective tumor suppressor gene, *BRCA1*-associated protein 1 (*BAP1*) is related to the occurrence of some malignant tumors such as UM (44). Studies have shown that loss of expression of nBAP1 is an important biomarker for the progression



and prognosis of UM (45). Therefore, *BAP1* immunohistochemical staining can be used to assess the risk of metastasis for UM (46). Besides, the elevation of serum markers such as LDH and alkaline phosphatase (ALP) is associated with shorter PFS and OS in UM patients. The expression changes of *IDO1* are related to the role of immune infiltrating cells in UM (47). The high expression of the long non-coding RNA (lncRNA) MIR155 host gene is associated with poor OS in UM patients and can be used to predict the efficacy of immune checkpoint inhibitor therapy (48). In this study, we constructed a new six-gene signature related to cancer hallmarks (including glycolysis and immune response). The survival analysis results confirmed that this six-gene signature, including *ARPC1B*, *BTBD6*, *GUSB*, *KRTCAP2*, *RHBDD3*, and *SLC39A4*, has good prognostic value for UM patients. It is worth mentioning that recent studies have established some prognostic gene signatures for UM as a supplement to traditional pathological staging. For example, a 10-gene signature established by Luo et al. showed excellent survival predictive ability for UM patients (23). We considered that a comparison of the survival predictive abilities of previously reported gene signatures and the six-gene signature will help to further explore the prognostic values of these gene signatures. Therefore, we compared the survival predictive abilities between the six-gene signature constructed in this study and the 10-gene signature previously reported by Luo et al. (23). The results showed that the two gene signatures had excellent survival predictive abilities in UM. The advantage of the six-gene signature is

that it had fewer genes. In addition, although Kaplan–Meier analysis indicates that the six-gene signature showed certain predictive ability in both SM and HCC, the ROC analysis suggested that the prognostic value of the six-gene signature in UM was much better than that in SM and HCC.

In addition, KEGG analysis indicated that the enrichment pathways of DEGs between the high-risk and low-risk groups included phagosome, Epstein–Barr virus infection, cell adhesion molecules, human T-cell leukemia virus 1 infection, human cytomegalovirus infection, cytokine–cytokine receptor interaction, tuberculosis, *S. aureus* infection, antigen processing and presentation, and Th1 and Th2 cell differentiation, suggesting that the role of the immune microenvironment in UM is worthy of further study. As is known, immunotherapy has become a hotspot in the field of tumor therapy in recent years. Exploration of the molecular mechanisms related to immune response in UM is expected to provide new methods to improve the effect of immunotherapy.

Previous studies have shown that *ARPC1B* is associated with T- and B-cell immunodeficiency. *ARPC1B* can be used not only as a predictive biomarker for assessing the sensitivity of UM to radiotherapy but also as a prognostic biomarker for oral squamous cell carcinoma (49, 50). *GUSB* participates in molecular pathways such as the innate immune system and can be used as a biomarker to predict lymph node metastasis in patients with early cervical cancer (51). *SLC39A4* can be used as a



## REFERENCES

- Aronow ME, Topham AK, Singh AD. Uveal Melanoma: 5-Year Update on Incidence, Treatment, and Survival (SEER 1973-2013). *Ocul Oncol Pathol* (2018) 4(3):145–51. doi: 10.1159/000480640
- Kaliki S, Shields CL. Uveal Melanoma: Relatively Rare But Deadly Cancer. *Eye (Lond)* (2017) 31(2):241–57. doi: 10.1038/eye.2016.275
- Yue H, Qian J, Yuan Y, Zhang R, Bi Y, Meng F, et al. Clinicopathological Characteristics and Prognosis for Survival After Enucleation of Uveal Melanoma in Chinese Patients: Long-Term Follow-Up. *Curr Eye Res* (2017) 42(5):759–65. doi: 10.1080/02713683.2016.1245422
- Dogrusoz M, Jager MJ. Genetic Prognostication in Uveal Melanoma. *Acta Ophthalmol* (2018) 96(4):331–47. doi: 10.1111/aos.13580
- Griewank KG, Koelsche C, van de Nes JAP, Schrimpf D, Gessi M, Moller I, et al. Integrated Genomic Classification of Melanocytic Tumors of the Central Nervous System Using Mutation Analysis, Copy Number Alterations, and DNA Methylation Profiling. *Clin Cancer Res* (2018) 24(18):4494–504. doi: 10.1158/1078-0432.CCR-18-0763
- Karydis I, Gangi A, Wheeler MJ, Choi J, Wilson I, Thomas K, et al. Percutaneous Hepatic Perfusion With Melphalan in Uveal Melanoma: A Safe and Effective Treatment Modality in an Orphan Disease. *J Surg Oncol* (2018) 117(6):1170–8. doi: 10.1002/jso.24956
- Lane AM, Kim IK, Gragoudas ES. Survival Rates in Patients After Treatment for Metastasis From Uveal Melanoma. *JAMA Ophthalmol* (2018) 136(9):981–6. doi: 10.1001/jamaophthalmol.2018.2466
- Zheng J, Irani Z, Lawrence D, Flaherty K, Arellano RS. Combined Effects of Yttrium-90 Transarterial Radioembolization Around Immunotherapy for Hepatic Metastases From Uveal Melanoma: A Preliminary Retrospective Case Series. *J Vasc Interv Radiol* (2018) 29(10):1369–75. doi: 10.1016/j.jvir.2018.04.030
- Rowcroft A, Loveday BPT, Thomson BNJ, Banting S, Knowles B. Systematic Review of Liver Directed Therapy for Uveal Melanoma Hepatic Metastases. *HPB (Oxford)* (2020) 22(4):497–505. doi: 10.1016/j.hpb.2019.11.002
- Gonsalves CF, Eschelmann DJ, Adamo RD, Anne PR, Orloff MM, Terai M, et al. A Prospective Phase II Trial of Radioembolization for Treatment of Uveal Melanoma Hepatic Metastasis. *Radiology* (2019) 293(1):223–31. doi: 10.1148/radiol.2019190199
- Khoja L, Atenafu EG, Suci S, Leyvraz S, Sato T, Marshall E, et al. Meta-Analysis in Metastatic Uveal Melanoma to Determine Progression Free and Overall Survival Benchmarks: An International Rare Cancers Initiative (IRCI) Ocular Melanoma Study. *Ann Oncol* (2019) 30(8):1370–80. doi: 10.1093/annonc/mdz176
- Rantala ES, Hernberg M, Kivela TT. Overall Survival After Treatment for Metastatic Uveal Melanoma: A Systematic Review and Meta-Analysis. *Melanoma Res* (2019) 29(6):561–8. doi: 10.1097/CMR.0000000000000575
- Carvajal RD, Schwartz GK, Tezel T, Marr B, Francis JH, Nathan PD. Metastatic Disease From Uveal Melanoma: Treatment Options and Future Prospects. *Br J Ophthalmol* (2017) 101(1):38–44. doi: 10.1136/bjophthalmol-2016-309034
- Bao R, Surriga O, Olson DJ, Allred JB, Strand CA, Zha Y, et al. Transcriptional Analysis of Metastatic Uveal Melanoma Survival Nominates NRP1 as a Therapeutic Target. *Melanoma Res* (2021) 31(1):27–37. doi: 10.1097/CMR.0000000000000701
- Li YZ, Huang Y, Deng XY, Tu CS. Identification of an Immune-Related Signature for the Prognosis of Uveal Melanoma. *Int J Ophthalmol* (2020) 13(3):458–65. doi: 10.18240/ijo.2020.03.14
- Carvajal RD, Piperno-Neumann S, Kapiteijn E, Chapman PB, Frank S, Joshua AM, et al. Selumetinib in Combination With Dacarbazine in Patients With Metastatic Uveal Melanoma: A Phase III, Multicenter, Randomized Trial (SUMIT). *J Clin Oncol* (2018) 36(12):1232–9. doi: 10.1200/JCO.2017.74.1090
- Krishna Y, McCarthy C, Kalirai H, Coupland SE. Inflammatory Cell Infiltrates in Advanced Metastatic Uveal Melanoma. *Hum Pathol* (2017) 66:159–66. doi: 10.1016/j.humpath.2017.06.005
- Figueiredo CR, Kalirai H, Sacco JJ, Azevedo RA, Duckworth A, Slupsky JR, et al. Loss of BAP1 Expression is Associated With an Immunosuppressive Microenvironment in Uveal Melanoma, With Implications for Immunotherapy Development. *J Pathol* (2020) 250(4):420–39. doi: 10.1002/path.5384
- Barbie DA, Tamayo P, Boehm JS, Kim SY, Moody SE, Dunn IF, et al. Systematic RNA Interference Reveals That Oncogenic KRAS-Driven Cancers Require TBK1. *Nature* (2009) 462(7269):108–12. doi: 10.1038/nature08460
- Liberzon A, Subramanian A, Pinchback R, Thorvaldsdottir H, Tamayo P, Mesirov JP. Molecular Signatures Database (MSigDB) 3.0. *Bioinformatics* (2011) 27(12):1739–40. doi: 10.1093/bioinformatics/btr260
- Langfelder P, Horvath S. WGCNA: An R Package for Weighted Correlation Network Analysis. *BMC Bioinf* (2008) 9:559. doi: 10.1186/1471-2105-9-559
- Tibshirani R. The Lasso Method for Variable Selection in the Cox Model. *Stat Med* (1997) 16(4):385–95. doi: 10.1002/(sici)1097-0258(19970228)16:4<385::aid-sim380>3.0.co;2-3
- Luo H, Ma C, Shao J, Cao J. Prognostic Implications of Novel Ten-Gene Signature in Uveal Melanoma. *Front Oncol* (2020) 10:567512. doi: 10.3389/fonc.2020.567512
- Park SY. Nomogram: An Analogue Tool to Deliver Digital Knowledge. *J Thorac Cardiovasc Surg* (2018) 155(4):1793. doi: 10.1016/j.jtcvs.2017.12.107
- Subramanian A, Tamayo P, Mootha VK, Mukherjee S, Ebert BL, Gillette MA, et al. Gene Set Enrichment Analysis: A Knowledge-Based Approach for Interpreting Genome-Wide Expression Profiles. *Proc Natl Acad Sci USA* (2005) 102(43):15545–50. doi: 10.1073/pnas.0506580102
- Heagerty PJ, Lumley T, Pepe MS. Time-Dependent ROC Curves for Censored Survival Data and a Diagnostic Marker. *Biometrics* (2000) 56(2):337–44. doi: 10.1111/j.0006-341x.2000.00337.x
- Chandran SS, Somerville RPT, Yang JC, Sherry RM, Klebanoff CA, Goff SL, et al. Treatment of Metastatic Uveal Melanoma With Adoptive Transfer of Tumour-Infiltrating Lymphocytes: A Single-Centre, Two-Stage, Single-Arm, Phase 2 Study. *Lancet Oncol* (2017) 18(6):792–802. doi: 10.1016/S1470-2045(17)30251-6
- Zhang H, Dai Z, Wu W, Wang Z, Zhang N, Zhang L, et al. Regulatory Mechanisms of Immune Checkpoints PD-L1 and CTLA-4 in Cancer. *J Exp Clin Cancer Res* (2021) 40(1):184. doi: 10.1186/s13046-021-01987-7
- Xu S, Tang L, Liu Z, Yang K, Cheng Q. Bioinformatic Analyses Identify a Prognostic Autophagy-Related Long Non-Coding RNA Signature Associated With Immune Microenvironment in Diffuse Gliomas. *Front Cell Dev Biol* (2021) 9:694633. doi: 10.3389/fcell.2021.694633
- Zhang Z, Ni Y, Chen G, Wei Y, Peng M, Zhang S. Construction of Immune-Related Risk Signature for Uveal Melanoma. *Artif Cells Nanomed Biotechnol* (2020) 48(1):912–9. doi: 10.1080/21691401.2020.1773480
- Stalhammar G, Seregard S, Grossniklaus HE. Expression of Immune Checkpoint Receptors Indoleamine 2,3-Dioxygenase and T Cell Ig and ITIM Domain in Metastatic Versus Nonmetastatic Choroidal Melanoma. *Cancer Med* (2019) 8(6):2784–92. doi: 10.1002/cam4.2167
- Pan H, Lu L, Cui J, Yang Y, Wang Z, Fan X. Immunological Analyses Reveal an Immune Subtype of Uveal Melanoma With a Poor Prognosis. *Aging (Albany NY)* (2020) 12(2):1446–64. doi: 10.18632/aging.102693
- Heppt MV, Steeb T, Schlager JG, Rosumek S, Dressler C, Ruzicka T, et al. Immune Checkpoint Blockade for Unresectable or Metastatic Uveal Melanoma: A Systematic Review. *Cancer Treat Rev* (2017) 60:44–52. doi: 10.1016/j.ctrv.2017.08.009
- Chan PY, Hall P, Hay G, Cohen VML, Szlosarek PW. A Major Responder to Ipilimumab and Nivolumab in Metastatic Uveal Melanoma With Concomitant Autoimmunity. *Pigment Cell Melanoma Res* (2017) 30(6):558–62. doi: 10.1111/pcmr.12607
- Kaunitz GJ, Cottrell TR, Lilo M, Muthappan V, Esandrio J, Berry S, et al. Melanoma Subtypes Demonstrate Distinct PD-L1 Expression Profiles. *Lab Invest* (2017) 97(9):1063–71. doi: 10.1038/labinvest.2017.64
- Johnson DB, Bao R, Ancell KK, Daniels AB, Wallace D, Sosman JA, et al. Response to Anti-PD-1 in Uveal Melanoma Without High-Volume Liver Metastasis. *J Natl Compr Canc Netw* (2019) 17(2):114–7. doi: 10.6004/jncn.2018.7070
- Heppt MV, Heinzerling L, Kahler KC, Forschner A, Kirchberger MC, Loquai C, et al. Prognostic Factors and Outcomes in Metastatic Uveal Melanoma Treated With Programmed Cell Death-1 or Combined PD-1/Cytotoxic T-Lymphocyte Antigen-4 Inhibition. *Eur J Cancer* (2017) 82:56–65. doi: 10.1016/j.ejca.2017.05.038
- Rabbie R, Ferguson P, Molina-Aguilar C, Adams DJ, Robles-Espinoza CD. Melanoma Subtypes: Genomic Profiles, Prognostic Molecular Markers and

- Therapeutic Possibilities. *J Pathol* (2019) 247(5):539–51. doi: 10.1002/path.5213
39. Sussman TA, Funchain P, Singh A. Clinical Trials in Metastatic Uveal Melanoma: Current Status. *Ocul Oncol Pathol* (2020) 6(6):381–7. doi: 10.1159/000508383
  40. Xin X, Zhang Y, Ling F, Wang L, Sheng X, Qin L, et al. Identification of a nine-miRNA Signature for the Prognosis of Uveal Melanoma. *Exp Eye Res* (2019) 180:242–9. doi: 10.1016/j.exer.2019.01.004
  41. Falzone L, Romano GL, Salemi R, Bucolo C, Tomasello B, Lupo G, et al. Prognostic Significance of Deregulated microRNAs in Uveal Melanomas. *Mol Med Rep* (2019) 19(4):2599–610. doi: 10.3892/mmr.2019.9949
  42. Starkey MP, Compston-Garnett L, Malho P, Dunn K, Dubielzig R. Metastasis-Associated microRNA Expression in Canine Uveal Melanoma. *Vet Comp Oncol* (2018) 16(1):81–9. doi: 10.1111/vco.12315
  43. Tang J, Wan Q, Lu J. The Prognostic Values of M6a RNA Methylation Regulators in Uveal Melanoma. *BMC Cancer* (2020) 20(1):674. doi: 10.1186/s12885-020-07159-8
  44. Bononi A, Giorgi C, Patergnani S, Larson D, Verbruggen K, Tanji M, et al. BAP1 Regulates IP3R3-Mediated Ca(2+) Flux to Mitochondria Suppressing Cell Transformation. *Nature* (2017) 546(7659):549–53. doi: 10.1038/nature22798
  45. Farquhar N, Thornton S, Coupland SE, Coulson JM, Sacco JJ, Krishna Y, et al. Patterns of BAP1 Protein Expression Provide Insights Into Prognostic Significance and the Biology of Uveal Melanoma. *J Pathol Clin Res* (2018) 4(1):26–38. doi: 10.1002/cjp.2.86
  46. Szalai E, Wells JR, Ward L, Grossniklaus HE. Uveal Melanoma Nuclear BRCA1-Associated Protein-1 Immunoreactivity Is an Indicator of Metastasis. *Ophthalmology* (2018) 125(2):203–9. doi: 10.1016/j.ophtha.2017.07.018
  47. Liang C, Peng L, Zeng S, Zhao Q, Tang L, Jiang X, et al. Investigation of Indoleamine 2,3-Dioxygenase 1 Expression in Uveal Melanoma. *Exp Eye Res* (2019) 181:112–9. doi: 10.1016/j.exer.2019.01.005
  48. Peng L, Chen Z, Chen Y, Wang X, Tang N. MIR155HG is a Prognostic Biomarker and Associated With Immune Infiltration and Immune Checkpoint Molecules Expression in Multiple Cancers. *Cancer Med* (2019) 8(17):7161–73. doi: 10.1002/cam4.2583
  49. Kumagai K, Nimura Y, Mizota A, Miyahara N, Aoki M, Furusawa Y, et al. Arpc1b Gene Is a Candidate Prediction Marker for Choroidal Malignant Melanomas Sensitive to Radiotherapy. *Invest Ophthalmol Vis Sci* (2006) 47(6):2300–4. doi: 10.1167/iovs.05-0810
  50. Auzair LB, Vincent-Chong VK, Ghani WM, Kallarakkal TG, Ramanathan A, Lee CE, et al. Caveolin 1 (Cav-1) and Actin-Related Protein 2/3 Complex, Subunit 1B (ARPC1B) Expressions as Prognostic Indicators for Oral Squamous Cell Carcinoma (OSCC). *Eur Arch Otorhinolaryngol* (2016) 273(7):1885–93. doi: 10.1007/s00405-015-3703-9
  51. Huang L, Zheng M, Zhou QM, Zhang MY, Jia WH, Yun JP, et al. Identification of a Gene-Expression Signature for Predicting Lymph Node Metastasis in Patients With Early Stage Cervical Carcinoma. *Cancer* (2011) 117(15):3363–73. doi: 10.1002/cncr.25870
  52. Ding B, Lou W, Xu L, Li R, Fan W. Analysis the Prognostic Values of Solute Carrier (SLC) Family 39 Genes in Gastric Cancer. *Am J Transl Res* (2019) 11(1):486–98.
  53. Wu DM, Liu T, Deng SH, Han R, Xu Y. SLC39A4 Expression is Associated With Enhanced Cell Migration, Cisplatin Resistance, and Poor Survival in non-Small Cell Lung Cancer. *Sci Rep* (2017) 7(1):7211. doi: 10.1038/s41598-017-07830-4
- Conflict of Interest:** The authors declare that the research was conducted in the absence of any commercial or financial relationships that could be construed as a potential conflict of interest.
- Publisher's Note:** All claims expressed in this article are solely those of the authors and do not necessarily represent those of their affiliated organizations, or those of the publisher, the editors and the reviewers. Any product that may be evaluated in this article, or claim that may be made by its manufacturer, is not guaranteed or endorsed by the publisher.
- Copyright © 2021 Liu, Lu and Li. This is an open-access article distributed under the terms of the Creative Commons Attribution License (CC BY). The use, distribution or reproduction in other forums is permitted, provided the original author(s) and the copyright owner(s) are credited and that the original publication in this journal is cited, in accordance with accepted academic practice. No use, distribution or reproduction is permitted which does not comply with these terms.